

# Coupled Geodesic Active Regions for Image Segmentation: A Level Set Approach

Nikos Paragios<sup>1</sup> and Rachid Deriche<sup>2</sup>

<sup>1</sup> Siemens Corporate Research,  
Imaging and Visualization Department,  
755 College Road East, Princeton, NJ 08540, USA  
E-mail: nikos@scr.siemens.com

<sup>2</sup> I.N.R.I.A.  
B.P. 93, 2004 Route des Lucioles,  
06902 Sophia Antipolis Cedex, France  
E-mail: der@sophia.inria.fr

**Abstract.** This paper presents a novel variational method for image segmentation that unifies boundary and region-based information sources under the Geodesic Active Region framework. A statistical analysis based on the Minimum Description Length criterion and the Maximum Likelihood Principle for the observed density function (image histogram) using a mixture of Gaussian elements, indicates the number of the different regions and their intensity properties. Then, the boundary information is determined using a probabilistic edge detector, while the region information is estimated using the Gaussian components of the mixture model. The defined objective function is minimized using a gradient-descent method where a level set approach is used to implement the resulting PDE system. According to the motion equations, the set of initial curves is propagated toward the segmentation result under the influence of boundary and region-based segmentation forces, and being constrained by a regularity force. The changes of topology are naturally handled thanks to the level set implementation, while a coupled multi-phase propagation is adopted that increases the robustness and the convergence rate by imposing the idea of mutually exclusive propagating curves. Finally, to reduce the required computational cost and the risk of convergence to local minima, a multi-scale approach is also considered. The performance of our method is demonstrated on a variety of real images.

## 1 Introduction

The segmentation of a given image is one of the most important techniques for image analysis, understanding and interpretation.

Feature-based image segmentation is performed using two basic image processing techniques: the **boundary-based segmentation** (which is often referred as edge-based) relies on the generation of a strength image and the ex-

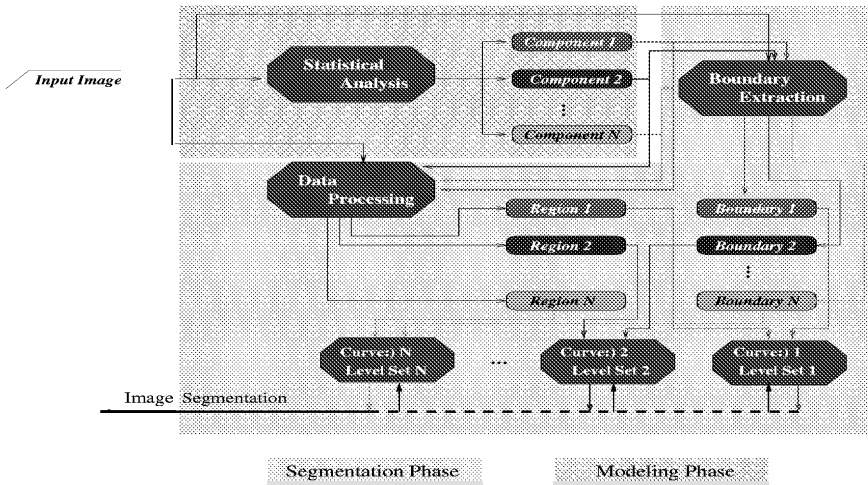


**Fig. 1.** Multi-phase Coupled Geodesic Active Regions for Image Segmentation: the flow chart.

traction of prominent edges, while the **region-based segmentation** relies on the homogeneity of spatially localized features and properties.

- Early approaches for **boundary-based** image segmentation have used local filtering techniques such as edge detection operators. However, such approaches have difficulty in establishing the connectivity of edge segments. This problem has been confronted by employing Snake/Balloons models [6, 12] which also require a good initialization step. Recently, the geodesic active contour model has been introduced [3, 13] which combined with the level set theory [14] deals with the above limitation resulting in a very elegant and powerful segmentation tool.
- The **region-based** methods are more suitable approaches for image segmentation and can be roughly classified into two categories: The region-growing techniques [2] and the Markov Random Fields based approaches [9]. The region growing methods are based on split-and-merge procedures using statistical homogeneity tests [7, 26]. Another powerful region-based tool, which has been widely investigated for image segmentation, is the Markov Random Fields (MRF) [10]. In that case the segmentation problem is viewed as a statistical estimation problem where each pixel is statistically dependent only on its neighbors so that the complexity of the model is restricted.
- Finally, there is a significant effort to **integrate boundary-based with region-based segmentation approaches** [4, 21, 26]. The difficulty lies on the fact that even though the two modules yield complementary information, they involve conflicting and incommensurate objectives. The region-based methods attempt to capitalize on homogeneity properties, whereas boundary-based ones use the non-homogeneity of the same data as a guide.

In this paper, a unified approach for image segmentation is presented that is based on the propagation of regular curves [4, 5, 23, 24, 26] and is exploited from the **Geodesic Active Region** model [19, 20]. This approach is as an extension of our previous work on supervised texture segmentation [18, 20].

This approach is depicted in [fig. (1)] and is composed of two stages. The first stage refers to a modeling phase where the observed histogram is approximated using a mixture of Gaussian components. This analysis is based on the Minimum Description Length criterion and the Maximum Likelihood Principle, denotes the regions number as well as their statistics, since a Gaussian component is associated to each region. Then, the segmentation is performed by employing the Geodesic Active Region model. The different region boundaries are determined using a probabilistic module that seeks for local discontinuities on the statistical space that is associated with the image features. This information is combined with the region one, resulting in a geodesic active region-based segmentation framework. The defined objective function is minimized with respect to the different region boundaries (multiple curves) using a gradient descent method, where the obtained equations are implemented using the level set theory that enables the ability of dealing automatically with topological changes. Moreover, as in [25, 5, 23], a coupling force is introduced to the level set functions that imposes the constraint of a non-overlapping set of curves. Finally, the objective function is used within the context of a coarse to fine multi-scale approach that increases the convergence rate and decreases the risk of converging to a local minimum.

The reminder of this paper is organized as follows. In section 2 the Geodesic Active Region model which is the basis of the proposed approach is shortly presented. The problem of determining the number of regions and their intensity properties is considered in section 3. The proposed segmentation framework is introduced in section 4, while its implementation issues are addressed in section 5. Finally, conclusions and discussion appear in section 6.

## 2 Geodesic Active Regions

The Geodesic Active Region [15] model was originally proposed in [16] to deal with the problem of supervised texture segmentation and was successfully exploited in [19] to deal with the the motion estimation and tracking problem.

This model will be shortly presented for a simple image segmentation case with two hypotheses ( $h_A, h_B$ ) (bi-modal). In order to facilitate the notation, let us make some definitions:

- Let  $I$  be the input frame.
- Let  $\mathcal{P}(\mathcal{R}) = \{\mathcal{R}_A, \mathcal{R}_B\}$  be a partition of the frame domain into two non-overlapping regions  $\{\mathcal{R}_A \cap \mathcal{R}_B = \emptyset\}$ .
- And, let  $\{\partial\mathcal{R}\}$  be the boundaries between  $\mathcal{R}_A$  and  $\mathcal{R}_B$ .

The Geodesic Active Region model assumes that for a given application some *information regarding the real region boundaries* and some *knowledge about the desired intensity properties of the different regions* are available. For example, let  $[p_C(I(s))]$  be the *boundary density function* that measures the probability of

a given pixel being at the boundaries between the two regions. Additionally, let  $[p_A(I(s)), p_B(I(s))]$  be the conditional intensity density functions with respect to the hypothesis  $h_A$  and  $h_B$ .

Then, the optimization procedure refers to a frame partition problem [determined by a curve that is attracted by the region boundaries] based on *the observed data, the associated hypotheses and their expected properties*. This partition according to the Geodesic Active Region model is given by:

$$\begin{aligned}
 E(\partial\mathcal{R}) = & \underbrace{\alpha \int_0^1 g \left( \underbrace{p_C(I(\partial\mathcal{R}(c)))}_{\text{boundary probability}} \right)}_{\text{Boundary Term}} \underbrace{|\partial\mathcal{R}(c)|}_{\text{regularity}} dc \\
 & + \underbrace{(1-\alpha) \iint_{\mathcal{R}_A} g \left( \underbrace{p_A(I(x,y))}_{h_A \text{ probability}} \right) dx dy}_{\mathcal{R}_A \text{ fitting measurement}} + \underbrace{(1-\alpha) \iint_{\mathcal{R}_B} g \left( \underbrace{p_B(I(x,y))}_{h_B \text{ probability}} \right) dx dy}_{\mathcal{R}_B \text{ fitting measurement}} \\
 & \underbrace{\hspace{10em}}_{\text{Region Term}}
 \end{aligned}$$

where  $\partial\mathcal{R}(c) : [0, 1] \rightarrow \mathcal{R}^2$  is a parameterization of the region boundaries in a planar form,  $\alpha \in [0, 1]$  is a positive constant balancing the contribution of the two terms, and  $g()$  is a positive monotonically decreasing function (*e.g.* Gaussian).

The interpretation of the above objective function is clear, since

**a curve is demanded**  $[\partial\mathcal{R}]$  **that:**

- is **regular** [regularity], of minimal length and is attracted by the real boundaries between the regions  $\mathcal{R}_A$  and  $\mathcal{R}_B$  [eq. (2): boundary attraction]: **Boundary Term**,
- and defines a partition of the image that optimizes the segmentation map by maximizing the *a posteriori* segmentation probability [20]: **Region Term**.

The minimization of this function is performed using a gradient descent method. If  $u = (x, y)$  is a point of the initial curve, then the curve should be deformed at this point using the following equation:

$$\frac{\partial u}{\partial t} = \left[ \underbrace{(1-\alpha) [g(p_A(I(u))) - g(p_B(I(u)))]}_{\text{region-based force}} + \underbrace{\alpha (g(p_C(I(u)))\mathcal{K}(u) - \nabla g(p_C(I(u))) \cdot \mathcal{N}(u))}_{\text{boundary-based force}} \right] \mathcal{N}(u)$$

The obtained PDE motion equation has two kind of *forces* acting on the curve, both in the direction of the normal inward normal,

– **Region force**

This force aims at shrinking or expanding the curve to the direction that maximizes the *a posteriori* segmentation probability according to the observation set and the expected intensity properties of the different regions.

– **Boundary force**

The force aims at shrinking the curve towards the boundaries between the different regions being constrained by the curvature effect.

### 3 Regions and their Statistics

In order to simplify the notation and to better and easily introduce the proposed model, let us make some definitions:

- Let  $H(I)$  be the observed density function (histogram) of the input image,
- Let  $\mathcal{P}(\mathcal{R}) = \{\mathcal{R}_i : i \in [1, N]\}$  be a partition of the image into  $N$  non-overlapping regions, and let  $\partial\mathcal{P}(\mathcal{R}) = \{\partial\mathcal{R}_i : i \in [1, N]\}$  be the region boundaries,
- And, let  $h_i$  be the segmentation hypothesis that is associated with the region  $\mathcal{R}_i$ .

The key hypothesis that is made to perform segmentation relies on the fact that the image is composed of homogeneous regions. In other words, we assume that the intensity properties of a given region (local histogram) can be determined using a Gaussian distribution and hence the global intensity properties of the image (image histogram) refer to a mixture of Gaussian elements.

Let  $p(\cdot)$  be the probability density function with respect to the intensity space of the image  $I$  (normalized image histogram  $H(I)$ ). If we assume that this probability density function is homogeneous, then an intensity value  $x$  is derived by selecting a component  $k$  with *a priori* probability  $P_k$  and then selecting this value according to the distribution of this element  $p_k(\cdot)$ . This hypothesis leads to a mixture model of Gaussian elements

$$p(x) = \sum_{k=1}^N P_k p_k(x), \quad p_k(x) = \frac{1}{\sqrt{2\pi}\sigma_k} e^{-\frac{(x-\mu_k)^2}{2\sigma_k^2}}$$

This mixture model consists of a vector  $\Theta$  with  $3N - 1$  unknown parameters  $\Theta = \{(P_k, \mu_k, \sigma_k) : k \in [1, \dots, N]\}$ : (i) The number of components  $[N]$ , (ii) the *a priori* probability of each component  $[P_k]$ , (iii) and, the mean  $[\mu_k]$  and the standard deviation  $[\sigma_k]$  of each component.

Hence, there are two key problems to be dealt with: the determination of the components number and the estimation of the unknown parameters  $\Theta$  of these components. These problems are solved simultaneously using the Minimum Description Length (MDL) criterion [22] and the Maximum Likelihood Principle (ML) [8]. Thus, given the data sample and all possible approximations using Gaussian Mixture models, the MDL principle is to select the approximation which minimizes the length of the mixture model as well as the approximation error using this model. In other words with more complex mixture models, the

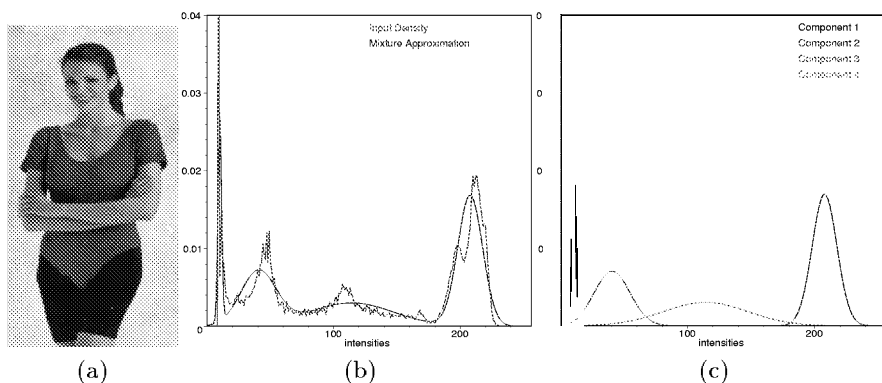


**Fig. 2.** (a) Input Image, (b) Image Histogram and its approximation: *Components Number: 4, Mean Approximation Error: 1.04641e-05, Iterations Number: 117*, (c) Region Intensity Properties [*Component 1: black pants, Component 2: background, Component 3: (hair, t-shirt), Component 4: skin*].

approximation is better and the error is minimized but at the same time the cost induced by the model is significant since more parameters are required for its description. Thus, a compromise between the components number and the approximation error has to be obtained.

This is done using the MDL principle, where initially a single node Gaussian mixture is assumed. Then, the number of mixture modes is increased and an estimation of the mixture parameters is performed. These parameters are used to determine the MDL measurement for the current approximation. If the obtained measurement is smaller than then one given by the approximation with a smaller number components, then the number of components is increased. Finally, the approximation the gives the minimum value for the MDL measurement is selected. The performance of this criterion is demonstrated in [fig. (2, 6)].

## 4 Image Segmentation

Given the region number as well their expected intensity properties, we can proceed to the segmentation phase. Two different modules are involved, a boundary and a region-based.

### 4.1 Determining the Boundary Information

The first objective is to extract some information regarding the real boundaries of each region. This can be done by employing an edge detector, thus by seeking for high gradient values on the input image. Given the hypothesis that this image is composed of homogeneous regions, this method will provide reliable global boundary information. However, this information is blind, since its nature cannot be determined. In other words, a pixel with important gradient value (boundary pixel) cannot be attributed to the boundaries of a specific region  $[\partial\mathcal{R}_i]$ .

Here, an alternative method is proposed to determine the boundary-based information [17]. Let  $s$  be a pixel of the image,  $N(s)$  a partition of its local neighborhood, and the  $N_R(s)$  and  $N_L(s)$  be the regions associated with this partition.

Moreover, let  $p_{B_k}(I(N(s)))$  be the boundary probability density function with respect to the  $k$  hypothesis,  $[p(I(N(s))|B_k)]$  be the conditional boundary probability and  $[p(I(N(s))|\bar{B}_k)]$  be the conditional non-boundary probability. Then, using the Bayes rule and making some assumptions regarding the global *a priori* boundary probability [17] it can be easily shown that the probability for a pixel  $s$  being at the boundaries of  $k$  region, given a neighborhood partition  $N(s)$  is given by,

$$p_{B_k}(s) = \frac{p(I(N(s))|B_k)}{p(I(N(s))|B_k) + p(I(N(s))|\bar{B}_k)}$$

The conditional boundary/non-boundary probabilities can be estimated directly from known quantities (see [17] for details). Thus,

**k Boundary Condition:**

If  $s$  is a  $k$  boundary pixel, then there is a partition  $[N_L(s), N_R(s)]$  where the most probable assignment for the “left” local region is  $k$  and for the “right”  $j$  [ $j \neq k$ ], or vice-versa,

**k Non-Boundary Condition:**

On the other hand, if  $s$  is not a  $k$  boundary pixel, then for every possible neighborhood partition the most probable assignment for the “left” as well as for the “right” local region is  $k$ , or  $i$  and  $j$  where  $\{i, j\} \neq k$ .

As a consequence, the conditional  $k$  boundary/non-boundary probability density functions are given by,

$$\begin{aligned} p(I(N(s))|B_k) &= \underbrace{p_k(I(N_R(s))) p_j(I(N_L(s)))}_{N_R(s) \in \mathcal{R}_k \cap N_L(s) \in \mathcal{R}_j} + \underbrace{p_j(I(N_R(s))) p_k(I(N_L(s)))}_{N_R(s) \in \mathcal{R}_j \cap N_L(s) \in \mathcal{R}_k} \\ p(I(N(s))|\bar{B}_k) &= \underbrace{p_k(I(N_R(s))) p_k(I(N_L(s)))}_{N_L(s) \in \mathcal{R}_i \cap N_R(s) \in \mathcal{R}_j} + \underbrace{p_i(I(N_R(s))) p_j(I(N_L(s)))}_{N_L(s) \in \mathcal{R}_k \cap N_R(s) \in \mathcal{R}_k} \end{aligned}$$

where  $\{i, j\}$  can be identical and

- $p_k(I(N_R(s)))$  is the probability of “right” local region  $[N_R(s)]$  being at the  $k$  region, given the observed intensity values within this region  $[I(N_R(s))]$ ,
- $p_j(I(N_L(s)))$  is the probability of “left” local region  $[N_L(s)]$  being at the  $j$  region, given the observed intensity values within this region  $[I(N_L(s))]$ .

Given the definition of the probability for a pixel  $s$  being a  $k$  boundary point, the next problem is to define the neighborhood partition. We consider four different partitions of the neighborhood and the local neighborhood regions are considered to be  $3 \times 3$  directional windows. We estimate the boundary probability for all partitions by using the mean values over these windows, and set the boundary information  $[p_{B,k}(s)]$  for the given pixel  $s$  with respect to the  $k$  using the partition with the maximum boundary probability. The same procedure is followed for all regions, given their intensity properties (Gaussian component) resulting on  $N$  boundary-based information images  $[p_{B,k}(s) : k \in [1, N]]$ . A demonstration of the extracted boundary information using this framework can be found in [fig. (3)].

## 4.2 Setting the Energy

The proposed method has made implicitly the assumption that the image is composed of  $N$  regions and a given pixel  $s$  lies always between two regions  $[\mathcal{R}_i, \mathcal{R}_{k_i}]$ . However, given the initial curves [regions] positions, some image pixels might not belong to any region. Moreover, other image pixels might be attributed to several regions.

To deal with this problem, a temporal *spending* region  $\mathcal{R}_0$  has to be considered. This region **(i) does not correspond to a real hypothesis** (it is composed from pixel with different hypotheses origins), **(ii) does not have a predefined intensity character** (it depends from the latest segmentation map) and **(iii) has to be empty when convergence is reached**. The next problem is to define the intensity properties of this region, thus the probability density function  $p_0()$ . This can be done by seeking the non-attributed image pixels and estimating directly from the observed intensity values the probability density function  $p_0()$ .

Then, the segmentation task can be considered within the geodesic active region framework where the region information is expressed directly from the Gaussian elements of the mixture model  $[p_i()]$  estimated in the observed image  $[p_i(I(s))]$ . Thus, the proposed framework consists of minimizing following objective function,

$$\left\{ \begin{array}{l} E(\mathcal{P}(\mathcal{R})) = \alpha \sum_{i=0}^N \iint_{\mathcal{R}_i} \underbrace{g(p_i(I(x, y)), \sigma_R)}_{\text{region fitting}} dx dy + \\ (1 - \alpha) \sum_{i=1}^N \int_0^1 \underbrace{g(p_{B,i}(\partial\mathcal{R}_i(c_i)), \sigma_B)}_{\text{boundary attraction}} \underbrace{|\partial\dot{\mathcal{R}}_i(c_i)|}_{\text{regularity constraint}} dc_i \end{array} \right.$$

where  $\partial\mathcal{R}_i(c_i)$  is a parameterization of the region  $\mathcal{R}_i$  boundaries into a planar form, and  $g(x, \sigma)$  is a Gaussian function.

Within this framework the set of the unknown variables consists of the different region boundaries (curves)  $[\partial\mathcal{R}_i]$ . The interpretation of the defined objective function is the same with the one presented in section 2 for the bi-modal Geodesic Active Region framework.

## 4.3 Minimizing the Energy

The defined objective function is minimized using a gradient descent method. Thus, the system of the Euler-Lagrange motion equations with respect to the different curves (one for each region) is given by:

$$\left\{ \begin{array}{l} \forall i \in [1, N], \\ \frac{\partial}{\partial t} \partial\mathcal{R}_i = \alpha \underbrace{[g(p_i(I(\partial\mathcal{R}_i)), \sigma_R) - g(p_{k_i}(I(\partial\mathcal{R}_i)), \sigma_R)] \mathcal{N}_i(\partial\mathcal{R}_i)}_{\text{Region-based force}} + \\ (1 - \alpha) \underbrace{(g(p_{B,i}(\partial\mathcal{R}_i), \sigma_B) \mathcal{K}_i(\partial\mathcal{R}_i) + \nabla g(p_{B,i}(\partial\mathcal{R}_i), \sigma_B) \cdot \mathcal{N}_i(\partial\mathcal{R}_i)) \mathcal{N}_i(\partial\mathcal{R}_i))}_{\text{Boundary-based force}} \end{array} \right.$$



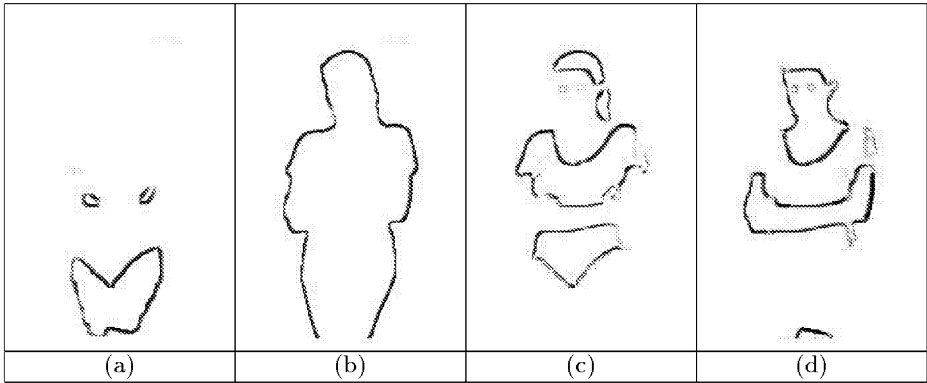


**Fig. 3.** Boundary information with respect to the different regions for the woman image [fig. (2.a)]. (a) *Region 1 (black pants)*, (b) *Region 2 (background)*, (c) *Region 3 (hair, t-shirt)*, (d) *Region 4 (skin)*.

where  $\mathcal{K}_i$  (resp.  $\mathcal{N}_i$ ) is the Euclidean curvature (resp. normal) with respect to the curve  $\partial\mathcal{R}_i$ .

Moreover, the assumption that **the pixel  $\partial\mathcal{R}_i$  lies between the regions  $\mathcal{R}_i$  and  $\mathcal{R}_{k_i}$  was done implicitly** to provide the above motion equations and the probability  $p_{k_i}(\cdot)$  is given by,

$$p_{k_i}(s) = \begin{cases} p_0(s), & \text{if } s \notin \cup_{j=1, j \neq i}^N [\mathcal{R}_j] \\ p_m(s), & m := \max \{p_m(s) : m \in [1, N], m \neq i, s \in \mathcal{R}_m\} \end{cases}$$

**Thus, if the given pixel is not attributed to any region, then the spending region distribution  $p_0(\cdot)$  is used to determine the  $k_i$  hypothesis. On the other hand, if this pixel is already attributed to one, or more than one regions, then the most probable hypothesis is used.**

These motion equations have the same interpretation with the one presented in section 2. Moreover, they refer to a **multi-phase curve propagation since several curves are propagated simultaneously**. In other words, each region is associated with a motion equation and the propagation of a single or multi-component initial curve. However, within this system of motion equations there is no interaction between the propagations of the different curves.

#### 4.4 Level Set Implementation

The obtained motion equations are implemented using the pioneering work of Osher and Sethian [14], the level set theory where the central idea is to represent the moving front  $\partial\mathcal{R}(c, t)$  as the zero-level set  $\{\phi(\partial\mathcal{R}(c, t), t) = 0\}$  of a function  $\phi$ . This representation of  $\partial\mathcal{R}(c, t)$  is implicit, parameter-free and intrinsic. Additionally, it is topology-free since different topologies of the zero level-set do not imply different topologies of  $\phi$ . It is easy to show, that if the moving front evolves according to  $[\frac{\partial}{\partial t} \partial\mathcal{R}(c, t) = F(\partial\mathcal{R}(c, t)) \mathcal{N}]$  for a given function  $F$ , then the embedding function  $\phi$  deforms according to  $[\frac{\partial}{\partial t} \phi(p, t) = F(p) |\nabla\phi(p, t)|]$  For this level-set representation, it is proved that the solution is independent of the

embedding function  $\phi$ , and in most of the cases is initialized as a signed distance function.

Thus, the system of motion equations that drives the multi-phase curve propagation for segmentation is transformed into a system of multiple surfaces evolution given by,

$$\left\{ \begin{array}{l} \forall i \in [1, N], \\ \frac{\partial}{\partial t} \phi_i(s) = \alpha (g(p_i(I(s)), \sigma_R) - g(p_{k_i}(I(s)), \sigma_D)) |\nabla \phi_i(s)| + \\ \quad (1 - \alpha) (g(p_{B,i}(s), \sigma_B) \mathcal{K}_i(s) |\nabla \phi_i(s)| + \nabla g(p_{B,i}(s), \sigma_B) \cdot \nabla \phi_i(s)) \end{array} \right.$$

#### 4.5 Coupling the Level Sets

The use of the level set methods provides a very elegant tool to propagate curves where their position is recovered by seeking for the zero level set crossing points. Moreover, the state of given pixel with respect to a region hypothesis can be easily determined since if it belongs to the region, then the corresponding level set value is negative. On the other hand if it does not belong to it, then the corresponding value is positive. Additionally, since we consider signed distance functions for the level set implementation, a step further can be done by estimating the distance of the given pixel from each curve. This information is very valuable during the multi-phase curve propagation cases where the overlapping between the different curves is prohibited.

However, the overlapping between the different curves is almost an inevitable situation at least during the initialization step. Moreover, the case where an image pixel has not been attributed to any hypothesis may occur. Let us now assume that a pixel is attributed initially to two different regions (there are two level set functions with negative values at it). Then, as in [25, 5, 23], a constraint that discourages a situation of this nature can be easily introduced, by **adding an artificial force (always in the normal direction)** to the corresponding level set motion equations that penalizes pixels with multiple labels (they are attributed to multiple regions). Moreover, a similar force can be introduced to discourage situations where pixels are not attributed to any regions. This can be done by modifying the level set motion equations as,

$$\left\{ \begin{array}{l} \forall i \in [1, N], \\ \frac{\partial}{\partial t} \phi_i(s) = \beta \underbrace{\sum_{j \in [1, N]} H_i(i, \phi_j(s)) |\nabla \phi_i(s)|}_{\text{Coupling force}} + \\ \quad \gamma \underbrace{[g(p_i(I(s)), \sigma_R) - g(p_{k_i}(I(s)), \sigma_R)] |\nabla \phi_i(s)|}_{\text{Region force}} + \\ \quad \delta \underbrace{\left( g(p_{B,i}(s), \sigma_B) \mathcal{K}_i(s) + \nabla g(p_{B,i}(s), \sigma_B) \cdot \frac{\nabla \phi_i(s)}{|\nabla \phi_i(s)|} \right) |\nabla \phi_i(s)|}_{\text{Boundary force}} \end{array} \right.$$

where  $\beta, \gamma, \delta$  are positive constants [ $\beta + \gamma + \delta = 1$ ], and the function  $H_i(\cdot, \phi(\cdot))$  is given by

$$H_i(m, \phi_n(s)) = \begin{cases} 0, & \text{if } m = i \\ -\text{sign}(\phi_j(s)), & \text{if } m \neq i \end{cases}$$

Let us now interpret the new artificial force that has been added to the motion equation  $i$ , for a given pixel  $s$ :

**Expanding Effect:**

If this pixel does not belong to any region, then the new force is negative, equal to  $f_c = -(N - 1)|\nabla\phi_i|$  and aims at expanding the region  $\mathcal{R}_i$  to occupy this pixel (the appearance of non-attributed pixels is discouraged).

**Shrinking Effect:**

On the other hand, if this pixel has been already attributed to another region  $[\mathcal{R}_k]$ , then the level set  $[\phi_k]$  will contribute with a positive force that aims at shrinking the region  $\mathcal{R}_i$  (the overlapping is discouraged).

Although the selection of the function  $[H_i(\phi(\cdot))]$  seems to fulfill the required conditions (mutually exclusive propagating curves, non overlapping, no “empty” pixels), it encounters some problems. Thus, the non-attributed pixels are penalized with the same manner to the ones that have been attributed to multiple regions. Finally, the defined coupling function is discontinuous which is a not desirable property since it creates stability problems during the level set evolution.

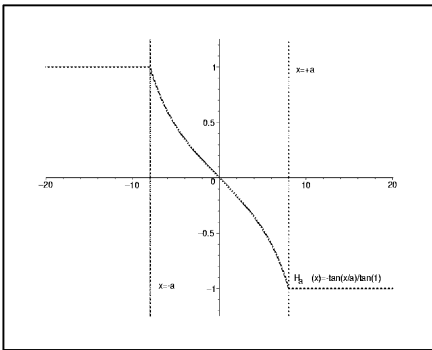


**Fig. 4.** The trigonometric basis of the level set coupling function.

To summarize, the coupling function has to be redefined by taking into account the following considerations:

- i. A pixel that is already attributed to a region  $j$  and is far away from  $\partial\mathcal{R}_j$ , should strongly discourage the evolution of the level set  $\phi_i(\cdot)$  to include this pixel in  $\mathcal{R}_i$ ,
- ii. A pixel which belongs to the region  $\mathcal{R}_j$  and is close to its boundaries can be reached or be liberated by  $\partial\mathcal{R}_j$  during the next few iterations, and hence, the coupling force introduced by the  $j$  level set function should “tolerate” a temporal overlapping.

Thus, inspired by the properties of the trigonometric functions, the coupling force is defined as,

$$H_i(j, \phi_j(s)) = \begin{cases} 0, & \text{if } j = i \\ H_\alpha(\phi_j(s)), & \text{if } j \neq i \text{ and } \phi_j(s) \geq 0 \\ \frac{1}{N-1} H_\alpha(\phi_j(s)), & \text{if } j \neq i \text{ and } [\bigcap_{k=1, k \neq i}^N \phi_k(s) > 0] \end{cases}$$

where the basis function  $H_a(x)$  is shown in [fig. (4)] and is given by:

$$H_a(x) = - \begin{cases} +1, & \text{if } x > a \\ -1, & \text{if } x < -a \\ \frac{1}{\tan(1)} \tan(x/a), & \text{if } |x| \leq a \end{cases}$$

In any case, the selection of this function is still an open issue and for the time being we are investigating other forms for it.

To interpret this force via the new function, a level set function  $[\underline{\phi}_i(\cdot)]$  and a pixel location  $[\underline{s}]$  are considered,

- i. If  $s$  is already attributed to another region, then there is an hypothesis  $j$  for which  $\phi_j(s) \leq 0$  which will contribute with a positive value (shrinking effect) to the coupling force that is proportional to the distance of this pixel from the boundaries of  $\mathcal{R}_j$ ,
- ii. A similar interpretation can be done if this pixel is not attributed to any region (expanding effect). However, for this case the coupling force has to be normalized because it is not appropriate to penalize with the same way the situation of overlapping and the case in which the given pixel is not attributed to one of the regions. At the same time this force is plausible if and only if this pixel is not attributed to any region  $[\bigcap_{\{k=1, k \neq i\}}^N \phi_k(s) > 0]$ .

## 5 Implementation Issues

However, analyzing the obtained motion equations, some hidden problems might be observed due to the fact that the region forces are estimated using a single intensity-based probability value. However, for real image segmentation cases there is always an overlap between the Gaussian components that characterize the different regions. Furthermore, due to presence of noise, isolated intensity values incoherent with the region properties can be found within it. As a consequence, it is quite difficult to categorize a pixel, based on its very local data (single intensity value).

To cope with these problems, a circular window approach can be used, as proposed in [26]. Hence, a centralized window is defined locally and the region-based force is estimated as the mean value of the region-based forces of the window pixels [fig. (5, 7, 8)]. However, here opposite to [26] where all the window pixels were equally considered, the distance between the window pixels and the window center is used, and these pixels contribute to the region with weights inversely proportional to their distances.

A more elegant solution can be obtained by considering a multi-scale approach. It is well known that the use of *multi-scale* techniques reduces significantly the required computational cost of the minimization process and performs a smooth operation to the objective function that reduces the risk of converging to local minima. The main idea consists in defining a consistent coarse-to-fine *multi-grid* contour propagation by using contours which are constrained to be piecewise constant over smaller and smaller pixel subsets [11]. The objective

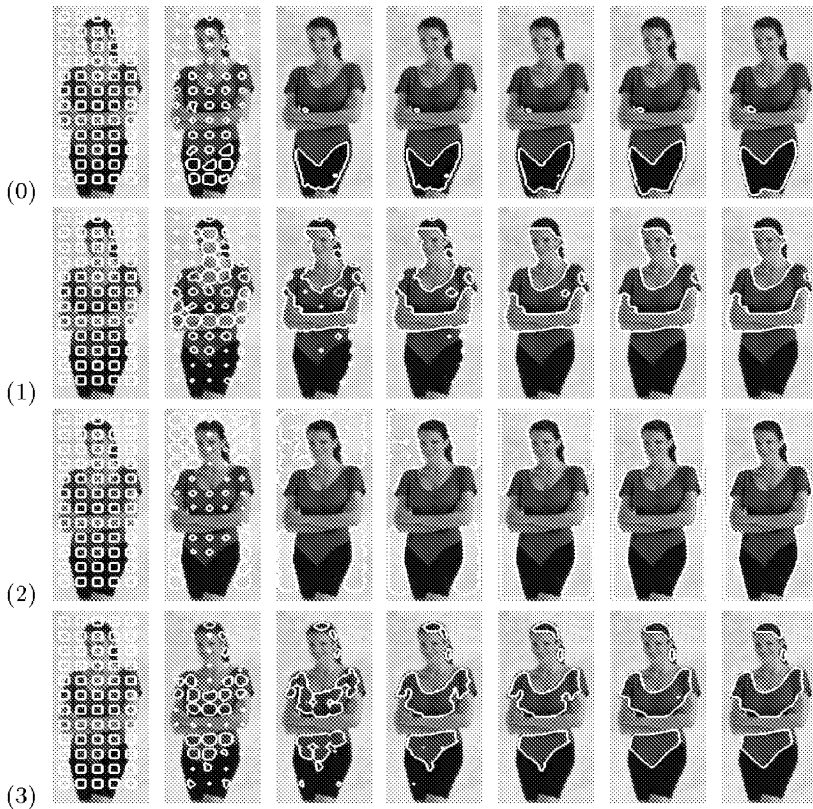


**Fig. 5.** Segmentation for the woman image [fig. (2.a)]. Multi-phase Curve Propagation. A random initialization step is used with a large number of spoiled regions. The initial regions are the same for all hypothesis. (1) *Region 1 (black pants)*, (2) *Region 2 (skin)*, (3) *Region 3 (background)*, (d) *Region 4 (hair, t-shirt)*.

function which is considered at each level is then automatically derived from the original finest scale energy function. Additionally, the finest data space is used at each level, and there is no necessity for constructing a multi-resolution pyramid of the data. More details about the multi-scale implementation of the proposed segmentation framework can be found at [17, 15].

As for the selection of the model parameters, we have observed that in most of the cases the region force is more reliable since it is estimated over blocks. On the other hand, the boundary force ensures the regularity of the propagating curves. Finally, the coupling force is considered less, with a progressive way since it has been introduced artificially and has a complementary role. Taking into account these remarks the following settings are used [ $\beta \approx 0.20$ ,  $\gamma \approx 0.35$ ,  $\delta \approx 0.45$ ]. Finally, as it concerns the  $\alpha$  parameter of the coupling function it is determined using the band size of the Narrow Band algorithm [1] which is used to implement the evolution of the level set functions.

To summarize, the proposed approach,

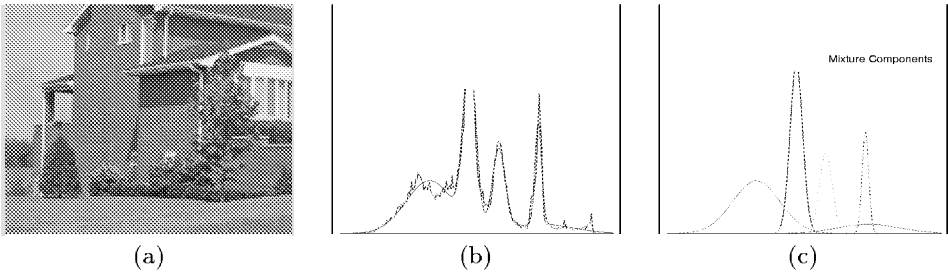


**Fig. 6.** (a) Input Image, (b) Image Histogram and its approximation: *Components Number: 5, Mean Approximation Error: 2.283931e-06, Iterations Number: 421*, (c) Region Intensity Properties.

- Initially, determines the number of regions and their intensity properties,
- Then, estimates the boundary-probabilities with respect to the different hypotheses,
- Finally, performs segmentation by the propagation of a “mutually exclusive” set of regular curves under the influence of boundary and region-based segmentation forces.

## 6 Discussion, Summary

In this paper<sup>1</sup>, a new multi-phase level set approach for un-supervised image segmentation has been proposed. Very promising experimental results were obtained using real images [fig. (5,7,8)] of different nature (outdoor, medical, etc.).

As far the computational cost of the proposed method is concerned (an ULTRA-10 Sun Station with 256 MB Ram and a processor of 299 MHZ was used) we can make the following remarks; the modeling phase is very fast almost real time. On the other hand, the segmentation phase is very expensive. The extraction of the boundary information takes approximately 3 to 5 seconds for a  $256 \times 256$  image with four different regions, while the propagation phase is more expensive due to the fact that there are multiple level set evolutions in parallel. Thus, for a  $256 \times 256$  image (Coronal image [fig. (8)]) with a random initialization step, the propagation phase takes approximately 20 seconds. However, this cost is strongly related with the regions number, the initial curve positions and the parameters of the level set evolution. This cost is significantly decreased by the use of the multi-scale approach (three to five times).

Summarizing, in this paper a new variational framework has been proposed to deal with the problem of image segmentation. The main contributions of the proposed image segmentation model are the following:

- An adaptive method that determines automatically the regions number and their intensity properties,

<sup>1</sup> A detailed version of this article can be found at [17], while more experimental results (in MPEG format) are available at:

<http://www-sop.inria.fr/robotvis/personnel/nparagio/demos>

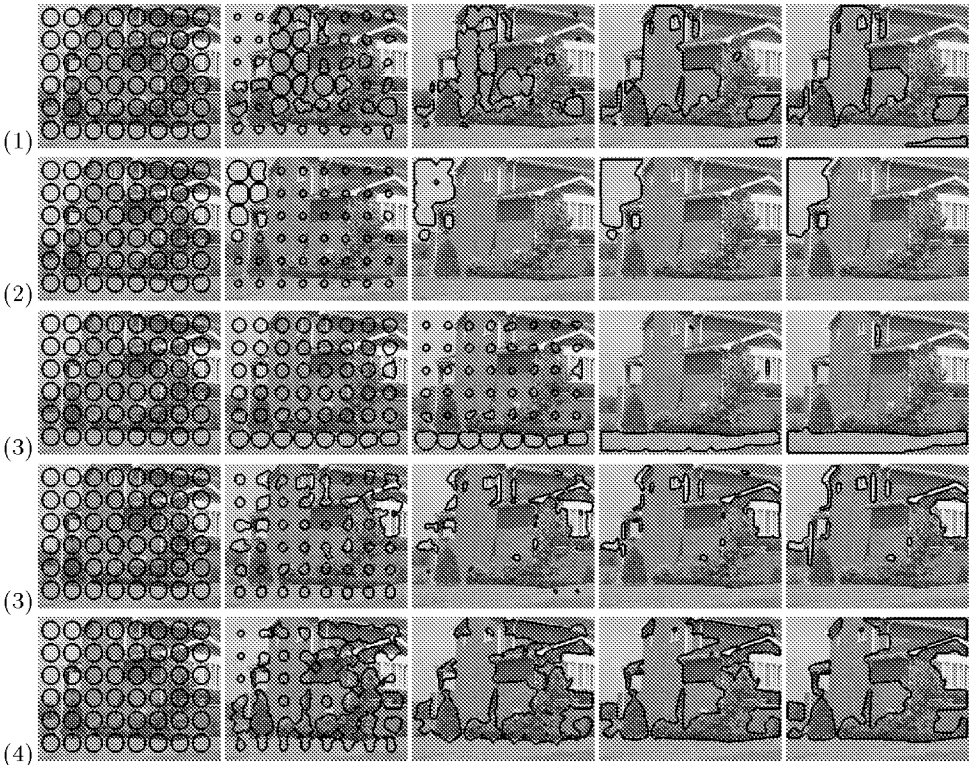


**Fig. 7.** The segmentation of the house image into five regions. Curve propagation: left to right. (a) House walls, (2) Sky, (b) Ground, (4) Windows, (5) Small trees, flowers, shadows.

- A variational image segmentation framework that integrates boundary and region-based segmentation modules and connects the optimization procedure with the the curve propagation theory,
- The implementation of this framework within level set techniques resulting on a segmentation paradigm that can deal automatically with changes of topology and is free from the initial conditions,
- The interaction between the different curves [regions] propagation using an artificial coupling force that imposes the concept of mutually exclusive propagating curves, increases the convergence rate, and eliminates the risk of convergence to a non-proper solution,
- And, the consideration of the proposed model in a multi-scale framework, which deals with the presence of noise, increases the convergence rate, and decreases the risk of convergence to a local minimum.

As far the future directions of this work, the incorporation to the model of a term that accounts for some prior knowledge with respect to expected segmentation map is a challenge (constrained geodesic active regions).

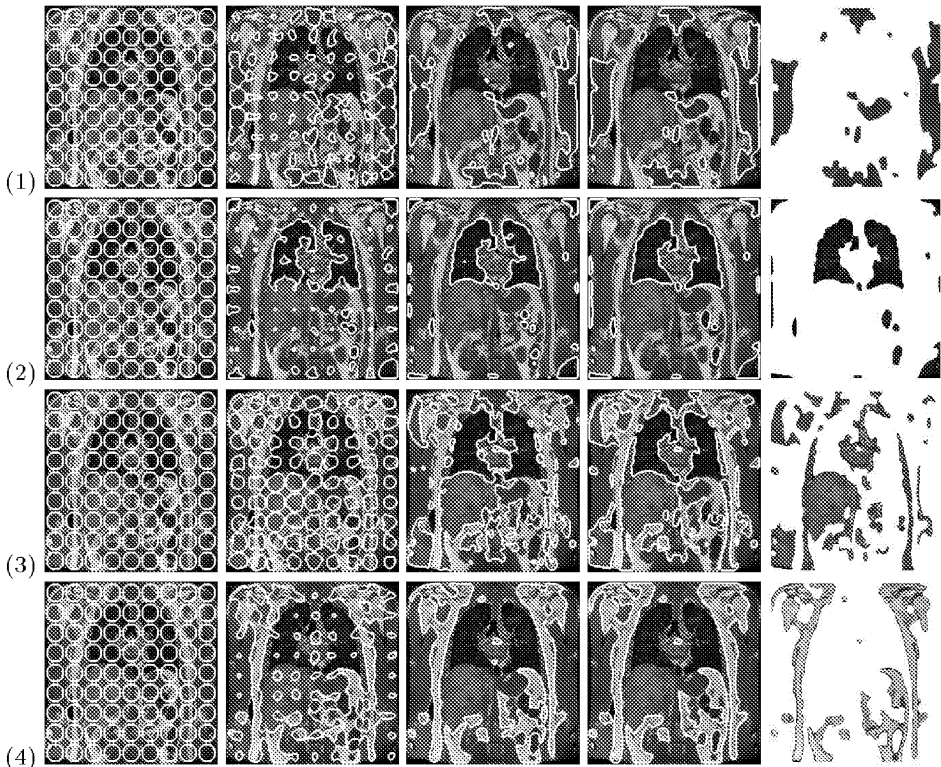


Fig. 8. Segmentation in five regions of a Coronal Medical image.

## Acknowledgments

This work has been carried out during the appointment (doctoral research) of the first author with the Computer Vision and Robotics Group (RobotVis) of I.N.R.I.A. Sophia Antipolis from October 1, 1996 to November 1, 1999 and was funded in part under the VIRGO research network (EC Contract No ERBFMRX-CT96-0049) of the TMR Program.

## References

1. D. Adalsteinsson and J. Sethian. A Fast Level Set Method for Propagating Interfaces. *Journal of Computational Physics*, 118:269–277, 1995.
2. R. Adams and L. Bischof. Seeded Region Growing. *IEEE Transactions on Pattern Analysis and Machine Intelligence*, 16:641–647, 1994.
3. V. Caselles, R. Kimmel, and G. Sapiro. Geodesic active contours. In *IEEE ICCV*, Boston, USA, 1995.
4. A. Chakraborty, H. Staib, and J. Duncan. Deformable Boundary Finding in Medical Images by Integrating Gradient and Region Information. *IEEE Transactions on Medical Imaging*, 15(6):859–870, 1996.
5. T. Chan and L. Vese. An Active Contour Model without Edges. In *International Conference on Scale-Space Theories in Computer Vision*, pages 141–151, 1999.



6. D. Cohen. On active contour models and balloons. *CVGIP: Image Understanding*, 53:211–218, 1991.
7. D. Comaniciu and P. Meer. Mean Shift Analysis and Applications. In *IEEE ICCV*, pages 1197–1203, Corfu, Greece, 1999.
8. R. Duda and P. Hart. *Pattern Classification and Scene Analysis*. John Wiley & Sons, Inc., 1973.
9. D. Geiger and A. Yuille. A common framework for image segmentation. *International Journal of Computer Vision*, 6:227–243, 1991.
10. S. Geman and D. Geman. Stochastic Relaxation, Gibbs Distributions, and the Bayesian Restoration of Images. *IEEE Transactions on Pattern Analysis and Machine Intelligence*, 6:721–741, 1984.
11. F. Heitz, P. Perez, and P. Bouthemy. Multiscale minimization of global energy functions in some visual recovery problems. *CVGIP: Image Understanding*, 59:125–134, 1994.
12. M. Kass, A. Witkin, and D. Terzopoulos. Snakes: Active contour models. *International Journal of Computer Vision*, 1:321–332, 1988.
13. S. Kichenassamy, A. Kumar, P. Olver, A. Tannenbaum, and A. Yezzi. Gradient flows and geometric active contour models. In *IEEE ICCV*, pages 810–815, Boston, USA, 1995.
14. S. Osher and J. Sethian. Fronts propagating with curvature-dependent speed : algorithms based on the hamilton-jacobi formulation. *Journal of Computational Physics*, 79:12–49, 1988.
15. N. Paragios. *Geodesic Active Regions and Level Set Methods: Contributions and Applications in Artificial Vision*. PhD thesis, University of Nice/ Sophia Antipolis, Jan. 2000.
16. N. Paragios and R. Deriche. Geodesic Active Regions for Texture Segmentation. Research Report 3440, INRIA, France, 1998. <http://www.inria.fr/RRRT/RR-3440.html>.
17. N. Paragios and R. Deriche. Coupled Geodesic Active Regions for image segmentation. Research Report 3783, INRIA, France, Oct. 1999. <http://www.inria.fr/RRRT/RR-3783.html>.
18. N. Paragios and R. Deriche. Geodesic Active Contours for Supervised Texture Segmentation. In *IEEE CVPR*, Colorado, USA, 1999.
19. N. Paragios and R. Deriche. Geodesic Active regions for Motion Estimation and Tracking. In *IEEE ICCV*, pages 688–674, Corfu, Greece, 1999.
20. N. Paragios and R. Deriche. Geodesic Active regions for Supervised Texture Segmentation. In *IEEE ICCV*, pages 926–932, Corfu, Greece, 1999.
21. T. Pavlidis and Y. Liow. Integrating region growing and edge detection. *IEEE Transactions on Pattern Analysis and Machine Intelligence*, 12:225–233, 1990.
22. J. Rissanen. Modeling by the Shortest Data Description. *Automatica*, 14:465–471, 1978.
23. C. Samson, L. Blanc-Feraud, G. Aubert, and J. Zerubia. A Level Set Model for image classification. In *International Conference on Scale-Space Theories in Computer Vision*, pages 306–317, 1999. <http://www.inria.fr/RRRT/RR-3662.html>.
24. A. Yezzi, A. Tsai, and A. Willsky. A Statistical Approach to Snakes for Bimodal and Trimodal Imagery. In *IEEE ICCV*, pages 898–903, Corfu, Greece, 1999.
25. H.-K. Zhao, T. Chan, and S. Osher. A variational level set approach to multiphase motion. *Journal of Computational Physics*, 127:179–195, 1996.
26. S. Zhu and A. Yuille. Region Competition: Unifying Snakes, Region Growing, and Bayes/MDL for Multiband Image Segmentation. *IEEE Transactions on Pattern Analysis and Machine Intelligence*, 18:884–900, 1996.